Nuclear Inst. and Methods in Physics Research, A 951 (2020) 163018

Contents lists available at ScienceDirect

Nuclear Inst. and Methods in Physics Research, A

journal homepage: www.elsevier.com/locate/nima

Energy response and identification efficiency of CsI(Tl) crystals irradiated with energetic protons

C. Frosin [a,b], S. Barlini [a,b,*], G. Poggi [a,b], G. Casini [b], M. Bini [a,b], A.A. Stefanini [a,b], S. Valdré [b], D. Gruyer [c], M. Ciemała [d], A. Maj [d], M. Ziebliński [d], B. Sowicki [d], K. Mazurek [d], N. Cieplicka-Oryńczak [d], M. Matejska-Minda [d], E. Bonnet [e], B. Borderie [f], R. Bougault [c], M. Bruno [g,h], A. Buccola [a,b], A. Camaiani [a,b], A. Chibhi [i], M. Cinausero [j], M. Cicerchia [k,j], J. Dueñas [l], D. Fabris [m], J. Frankland [i], F. Gramegna [j], M. Henri [i], A. Kordyasz [n], T. Kozik [o], N. Le Neindre [c], I. Lombardo [p], O. Lopez [c], G. Mantovani [k,j], T. Marchi [j], A. Olmi [b], P. Ottanelli [a,b], M. Parlog [c,q], S. Piantelli [b], G. Pasquali [a,b], S. Upadhyahya [o], G. Verde [p], E. Vient [c]

[a] Dipartimento di Fisica, Università di Firenze, I-50019 Sesto Fiorentino, Italy
[b] INFN Sezione di Firenze, I-50019 Sesto Fiorentino, Italy
[c] LPC Caen, ENSICAEN, Université de Caen, CNRS-IN2P3, F-14050 Caen cedex, France
[d] Institute of Nuclear Physics, Polish Academy of Science, PL-31342, Krakow, Poland
[e] Université Nantes, EMN IN2P3 CNRS, SUBATECH, Nantes, France
[f] IPNO, CNRS-IN2P3, Université Paris-Sud 11, F-91406 Orsay cedex, France
[g] Dipartimento di Fisica, Università di Bologna, I-40126 Bologna, Italy
[h] INFN Sezione di Bologna, I-40126 Bologna, Italy
[i] GANIL, CEA/DSM-CNRS/IN2P3, F-14076 Caen cedex, France
[j] INFN Laboratori Nazionali di Legnaro, I-35020 Legnaro, Italy
[k] Dipartimento di Fisica, Università di Padova, I-35131 Padova, Italy
[l] Depto. de Ing. Eléctrica y Centro de Estudios Avanzatos en Física, Matemáticas y Computación, Universidad de Huelva, S-21071 Huelva, Spain
[m] INFN Sezione di Padova, I-35131 Padova, Italy
[n] Heavy Ion Laboratory, University of Warsaw, PL-02093, Warsaw, Poland
[o] Phys. Astr. and Appl. Comp. Sci., Jagellionan University, PL-30348, Krakow, Poland
[p] INFN Sezione di Catania, I-95123 Catania, Italy
[q] Horia Hulubei, IFIN-HH, RO-077125 Bucarest Magurele, Romania

ARTICLE INFO

MSC:
00-01
99-00

Keywords:
CsI(Tl) detectors
Particle identification method
Light-energy response
Heavy ion collisions

ABSTRACT

The proton energy calibration and the corresponding identification efficiency of the Thallium activated Cesium Iodide (CsI(Tl)) crystals of the FAZIA detection system have been studied in the range of 59–180 MeV by using the proton beam delivered by the cyclotron of the CCB (Cyclotron Center Bronowice) facility. The light output versus energy is linear in the lower portion of the investigated energy range while showing a deviation from linearity on the higher energy side. The effects of proton induced nuclear collisions have been identified and estimated via Pulse Shape Analysis in CsI(Tl) crystals. Experimental efficiency for proton identification in the examined energy range is deduced and compared with GEANT4 simulations. For a well collimated crystal, and at the highest considered energy, the efficiency value comes out to be about 70%.

1. Introduction

Inorganic scintillators and in particular CsI(Tl) are essential parts of many detector setups in nuclear physics. The literature reports on a large number of applications where these crystals are used as the last layer of detector stacks in telescope configuration because of their high stopping power (see for example Refs. [1–6]). High quality crystals grown with the necessary good control of the dopant concentration (typical range from 1000 to 2000 ppm) and homogeneity are available and they are coupled with either photomultiplier tubes or silicon photodiodes. The energy measured by the crystals can be used together with the energy released in the previous telescope layer(s) to obtain Particle Identification (PID) via the well known ΔE–E method. Moreover, the scintillation produced in CsI(Tl) shows two main components, commonly labeled as *fast* and *slow*. The decay constant ($\tau \sim 0.5$-1 μs) and the amplitude of the fast component depend, for a given

* Correspondence to: via Sansone 1, 50019 Sesto Fiorentino (FI), Italy.
E-mail address: barlini@fi.infn.it (S. Barlini).

https://doi.org/10.1016/j.nima.2019.163018
Received 24 July 2019; Received in revised form 18 October 2019; Accepted 20 October 2019
Available online 31 October 2019
0168-9002/

deposited energy, on the particle type [7]. For a particle fully stopped in the scintillator, this property is exploited for PID via Pulse Shape Analysis (PSA) which, in our case, allows event-by-event charge and mass identification of light charged particles up to Boron isotopes.

One of the drawbacks of the CsI(Tl) detectors is the non-linear dependence of the light response on the deposited particle energy. This non-linearity, mainly observed at low incident energy, depends on mass and charge of the impinging ion and increases with increasing stopping power, being partially referable to quenching effects [8]. The effect is evident only for impinging particles with Z larger than 1. Several formulas and procedures have been suggested to express the light output as a function of energy [8–13].

In this paper we report on an experiment designed to study the response to protons of the CsI(Tl) crystals used in the FAZIA apparatus, a modular detector array based on a three stage silicon (Si1)-silicon (Si2)-CsI(Tl) telescope [1]. The goal of the experiment was twofold. Firstly, we wanted to perform the energy calibration of the crystals using protons at the highest measurable energies, thus possibly checking the existence of non-linear effects in the crystals. Secondly, we wanted to study the identification efficiency of the CsI(Tl) crystals at energies greater than 100 MeV, where protons traveling in thick detectors can experience interactions (Coulomb or nuclear elastic scattering and reactions) which, as described later on, can produce events characterized by an Incomplete Energy Deposition (IED). The *identification efficiency* of the crystal is given by the percentage of properly identified protons (in terms of charge, mass and energy) with respect to the total number of impinging protons. The calibration for high energy protons and their identification efficiency are necessary for a correct analysis of the data collected during the FAZIA campaign started in GANIL, where a significant fraction of high energy protons is expected as secondary products of the heavy ion collisions at beam energies even higher than 50 MeV/n.

The layout of this paper is the following. Section 2 describes the experimental set-up, while Section 3 discusses the energy calibration. The study of IED events is reported in Section 4. The evaluation of the proton efficiency as a function of energy is shown in Section 5, where a comparison with a GEANT4 simulation is also reported.

2. Experimental set-up

The measurements were performed at the Cyclotron Center Bronowice (CCB) at Kraków (Poland) where an experimental area is dedicated to fundamental and applied research. The experimental set-up is shown in Fig. 1. The proton beam (typical current ≈20 nA) impinged on a ^{nat}Ti foil (4 cm diameter, 6.8 mg/cm ^{2} thickness) placed at the center of the scattering chamber.

The CCB cyclotron permits to vary the proton energy in a few minutes from 230 MeV down to the minimum energy of 70.3 MeV. For our experiment, the maximum used energy was 180 MeV, near the punch through value for the FAZIA crystals (194 MeV). To extend the energy range down to 59 MeV, Aluminum degraders were placed in front of the detectors. For this test, we mounted two FAZIA telescopes in their standard configuration, consisting of two layers of silicon detectors followed by a CsI(Tl) scintillator. In the present experiment, both silicons were 500 μm thick in order to increase the energy deposited in the ΔE signal. Details of the FAZIA detection system are found in Ref. [1,14,15].

These crystals have a shape close to that of a parallelepiped, with a slight tapering required by the design distance from the target (100 cm). The front area is 20.4 × 20.4 mm^2, the rear one is 21.7 × 21.7 mm^2 and the thickness is 100 mm. Their front face is protected by a reflecting aluminized Mylar foil (1.5 μm thick) while the lateral wrapping consists of high reflecting polymer foil (ESR Vikuiti, 3M) covered by an opaque tape. The readout is done by a custom photodiode with 18 × 18 mm^2 active area produced by the CIS company[1] coupled to the crystal with an optical cement with a refraction index n≈1.4.

The telescopes were mounted on an equatorial plane in the vacuum chamber at a distance of 44 cm from the target. During the experiment, the two FAZIA telescopes (F1 and F2 in the following) have been tested in different configurations in terms of angular position and set-up (collimated and not). In particular, the collimated set-up has been obtained using a 42 mm thick iron block with a circular hole (5 mm diameter). The chosen thickness of the collimators was such as to stop protons at the planned highest beam energy.

Apart from the charge preamplifiers (see below), the electronics used for the test is fully digital and it is the same used by the FAZIA apparatus, described elsewhere [14,15]. Charge preamplifiers are connected to the Silicon detectors and to the photodiodes. Their main characteristics are a high dynamic range and a fast response (few ns risetime). The preamplifiers are based on the layout of an earlier design [16] where also a current amplification section was included, implemented only during the R&D phase of FAZIA. High dynamic range and fast risetime are necessary in order to comply with the demanding PSA performed on Silicon and CsI(Tl) signals. In this experiment, the trigger is generated by the CsI(Tl) crystals. In the following, when a ΔE–E correlation is shown, a threshold on the sum of the energy deposited in Si1 and Si2 is applied to show only amplitudes above the noise level. This corresponds to consider only interactions of charged particles in CsI(Tl) having deposited energy in the Silicon detectors, thus excluding events associated with neutron and gamma-rays detection in the crystal. The waveforms of all silicon and CsI(Tl) detectors are continuously sampled and shaped via digital trapezoidal filters with unit gain, whose maximum value provides the light output information expressed in terms of ADC units (ADU) of the sampler. Once the trigger is validated, the maximum amplitude of each shaper is acquired. The parameters of the filters differ for the various detectors. In particular, for the silicon detectors a rise-time of 2 μs and a flat top of 1 μs are chosen. For CsI(Tl) signals, two shapers are active: the first one, with a rise-time of 2 μs and a flat top of 0.5 μs, is more sensitive to the *fast* component. The second one has a rise-time of 2 μs and a flat top of 10 μs in order to be sensitive to the sum of the two components and to minimize the ballistic effect, i.e. an amplitude deficit depending on the time evolution of the signal. In the following the amplitudes of the first and the second shaper are referred to as *FLO* (Fast Light Output) and *LO* (Light Output), respectively. We consider *LO* as the correct total light output estimation of the CsI(Tl), directly connected to the energy deposited by the impinging particles.

3. CsI(Tl) energy calibration with proton beam

Within the FAZIA collaboration, the energy calibration in CsI(Tl) for lower energy protons, as well as for other particles, is usually performed by using the formula developed in [9,10] and exploiting the information of the energy deposited in the silicon detectors. The method cannot be used if the energy released in the silicon detector is so low that the uncertainty associated with the electronic noise and/or straggling jeopardizes the procedure. This happens for proton energies higher than a few tens of MeV and, as anticipated in Section 1, the purpose of the present experiment is indeed to find an energy calibration of the scintillator applicable to this high-energy region, where the procedure applicable to the lower energy fails.

In the already described experimental setup, protons elastically scattered by the target represent only a fraction of the detected events because other contributions arise from reactions in the target and from side effects associated with the presence of the iron collimator. In particular, a specially developed GEANT4 simulation shows that a sizeable contribution comes from protons scattered near the entrance of collimator. All these effects, while contributing to form an extended

[1] www.cismst.org.

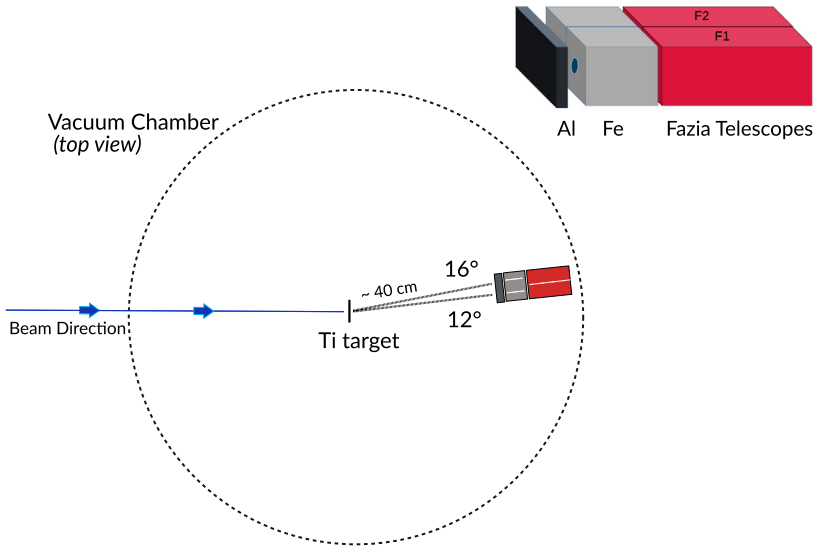

Fig. 1. Layout of the experimental set-up. The iron collimators (Fe) and the aluminum (Al) absorber are shown. They are placed in front of the two FAZIA telescopes during part of the operation — see text for details.

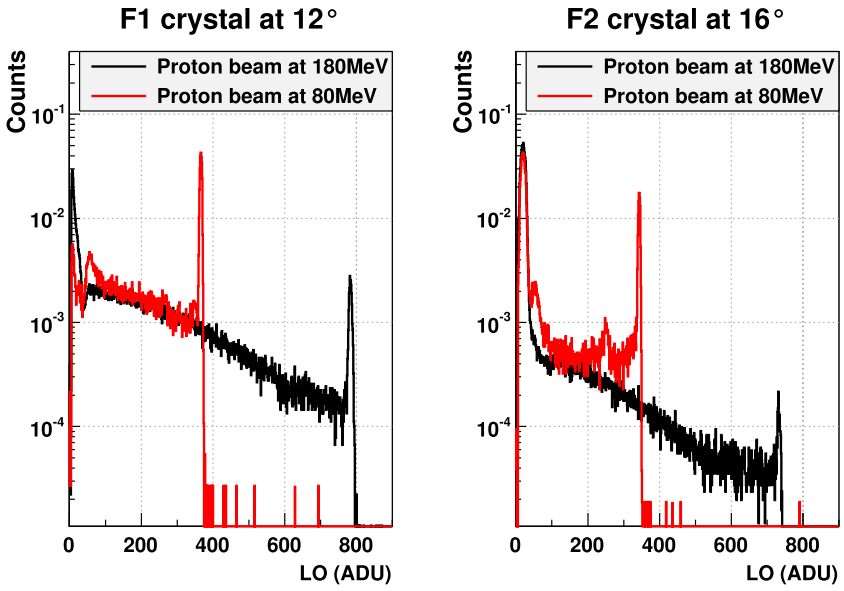

Fig. 2. (Color online) Proton Light Output (LO) spectra expressed in ADC unit (ADU), measured with the two FAZIA CsI(Tl) in the collimated configuration at two beam energies. Left: detector F1 placed at 12° with respect to the beam direction; Right: detector F2 placed at 16° with respect to the beam direction. The histogram areas are normalized to 1.

low-energy tail in the measured proton spectra, do not prevent the detection of the sharp elastic peak needed for the energy calibration. Fig. 2 shows the proton energy spectra for F1 and F2 in collimated geometry, at beam energies of 80 and 180 MeV, for the small polar angle configuration. The elastic peaks clearly emerge. The resulting energy resolution for the F1 crystal is 1.7% (1.2%) for 80 MeV (180 MeV) stopped protons, while for the F2 crystal slightly larger values are obtained. In the following sections, the correlations ΔE–E and PSA are presented for the F2 telescope, because the energy resolutions of the relevant silicon detectors were better than those of F1.

As already mentioned, the CsI(Tl) light output is non-linear with respect to the energy released by the radiation in a way which depends on the ion mass A and charge Z. Limiting to protons, previous studies indicate that the CsI(Tl) response can be considered linear down to the 1 MeV region [9,10,17,18]. According to recently reported measurements [19] for the CsI(Tl) of the HIRA10 apparatus, while linearity is maintained for proton energy even lower than 1 MeV (see Fig. 7 of [19]), an unexpected non-linearity appears at high energy, close to the punch-through value of their 10 cm long crystals (see Fig. 11 of [19]).

Coming to our data, the upper panel of Fig. 3 shows, for the F1 crystal, the measured *LO* vs. energy for protons. The points are the experimental results while the two lines are results of the fit discussed below. Please note that the linear fit was applied only for protons of an energy lower than 110 MeV, i.e. to the region where linearity is present, as discussed shortly. All the parameters resulting from the fits are reported in Tables 1 and 2. The proton energies range from the minimum of about 59 MeV (beam energy 80 MeV with 9 mm Al degraders) to 180 MeV. As far as errors are concerned, the peak

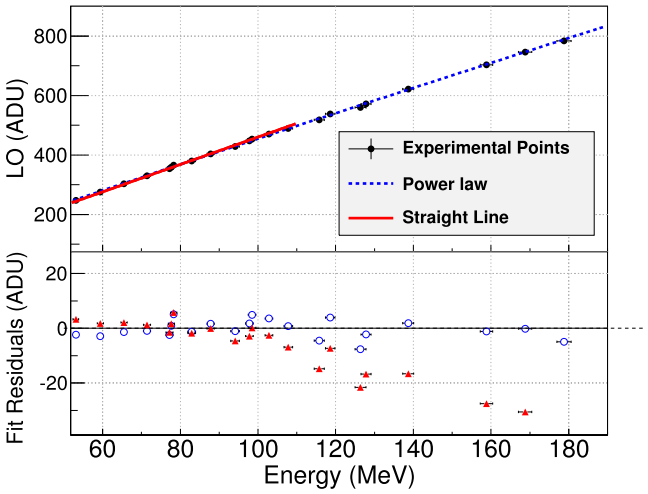

Fig. 3. (Color on line) Upper panel: experimental correlation between the Light Output (*LO*) expressed in ADC unit (ADU) and the proton energy (black points) for the F1 crystal. The red line represents a linear fit of the experimental points below 110 MeV while the blue dotted line is a power law fit applied on the whole set of data (see text). Bottom panel: residuals of the two fits (red triangles: linear fit, blue open dots: power law). Note that for the linear fit the residuals are presented also for experimental points non included in the fit. Uncertainties are discussed in the text.

position of the elastically scattered protons has been obtained from a Gaussian fit and only the statistical errors are considered (typically 0.5 ADU). The beam energy is known with a nominal accuracy of ±1%. The energy for scattered protons is calculated for a deflection angle corresponding to the center of the detector. The variation of the proton energy with the polar angle for the elastic scattering on Ti is anyway very weak, below 0.3 MeV for a 4° variation, so that the associated uncertainty is well below the beam energy accuracy. For the lower energies, reached with the Al degraders, the accuracy of the energy-loss calculations (typically 2–3%) has been considered. As a consequence, the uncertainty increases from 1% at 180 MeV to 1.5% at 60 MeV. As far as the functional forms of the *LO* vs energy calibration is concerned, we remind that they must have the property of passing through the origin, because our digital treatment of the signals and of the baseline subtraction [20,21] guarantees the absence of a significant offset and deviation from linearity (if any) is very small and confined in a narrow region well below 1 MeV. Indeed, the linear fit passing through the origin (red continuous line) well describes all the measured energies in the lower energy region, while one observes a systematically increasing deviation from a straight line for an energy higher that about 110 MeV. This is particularly evident in the bottom panel of Fig. 3 where the residuals in ADU units (red triangles for the linear fit) are shown even for points not included in the fit. This observation is quite in agreement with the findings reported in [19]. A possible explanation of the observed non-linearity could be associated with the tapering (see for instance Ref. [22]) of the crystals adopted by both the HiRA10 and Fazia apparatus. Some preliminary tests on the CsI(Tl) of Fazia with gamma sources and GEANT4 simulations confirm this interpretation. We will address this topic in a dedicated future paper. In any case, the best fit in the *LO* vs. energy correlation of our data is obtained using the simple expression $LO = aE^b$ with a and b as free parameters. Although many different functional forms for fitting the results could be chosen, we decided to adopt the same approach used (and justified) in [19] for addressing the same problem. The results are shown in the upper panel of Fig. 3 as a blue dotted line for the F1 crystal. The improvement is better appreciated by looking at the residuals (blue open dots, bottom panel). The reduced χ^2 value confirms this improvement. The χ^2 values obtained for the power law fit point to a possible overestimation of the beam energy uncertainty adopted in the fit. It is remarkable that the value of the exponent b is the same within errors for the two Fazia crystals, as expected for nominally identical crystals prepared according the same procedure. Moreover, it is to be noted that the exponent obtained from the fit is close to the value reported in [19], supporting the hypothesis of a common origin, like the crystal tapering present in all the considered crystals.

Table 1
Fit values obtained with the $LO = mE$ formula for the two Fazia crystals. NDF represents the number of degrees of freedom. Please note that the fit is applied only to proton energies lower than 110 MeV.

$LO = mE$	m (ADU/MeV)	χ^2/NDF
F1	4.60 ± 0.01	7.9/13
F2	4.30 ± 0.01	10.4/13

Table 2
Fit values obtained with the $LO = a * E^b$ formula for the two Fazia crystals. The fit is applied to the whole set of proton energies.

$LO = aE^b$	a (ADU/MeV)	b	χ^2/NDF
F1	5.91 ± 0.02	0.94 ± 0.01	9.5/19
F2	5.52 ± 0.02	0.94 ± 0.01	14.4/19

The data presented in this section exploit all the used configurations (collimated and uncollimated) and, as a matter a fact, no evidence has been found for differences in the behavior between the two configurations. In the following sections data will refer only to the collimated geometry.

4. Study of the proton incomplete energy deposition using PSA

The impinging particle, before being stopped in CsI(Tl), can undergo interactions, that can be either elastic scattering or reactions. The effects due to nuclear reactions in CsI(Tl) are well known (see for instance [23,24]). They are expected to contribute in various manners to the final signal amplitude in the crystal. For instance, inelastic scattering reduces the energy deposited by the particle; similarly, a smaller energy deposition results when neutrons are present in the exit channel or when secondary charged particles are produced. In the latter case, the reduction of the light output is due to quenching effects which increase with charge and mass of the secondary particles. The effects due to the elastic scattering processes are usually disregarded, because their importance strongly depends on the shape of the detector, which the particles might escape from. For instance, the losses due to elastically scattered protons were not considered in [23] because the transverse dimension of the used CsI(Tl) crystals was either equal or significantly larger than the longitudinal one. In our case as well as in [19], the geometry of the crystals is quite different and an elastically deflected proton may escape from the detector: in this case the energy loss process in the crystal is interrupted before the particle stops. As a consequence of all these effects, part of the original energy is not released in the crystal and this results in an IED (Incomplete Energy Deposition) event. It is worth noting that we are able to study these effects also exploiting the PSA in the relevant detector, while in the other cited examples [23,24] only the information about the energy deposited in the crystal was available. In particular, for most of the IED events a different combination of *FLO* and *LO* components is expected with respect to stopped particles: the measurable effect in terms of PSA significantly helps to pin down the correct interpretation of the data, as discussed in the next Section. In the standard $\Delta E(Si) - E(CsI)$ correlations, the IED events are characterized by a correct energy deposition in the Si layer(s) and by an incorrect (i.e. lower that expected) energy deposition in the CsI(Tl) layer. In heavy ion experiments, this is particularly evident for hydrogen and helium nuclei, which are the most abundant and penetrating reaction products. As a matter of fact, a low energy tail appears below the ridges of p,d,t and alpha particles. Good examples of this behavior can be found in Fig. 7 of Ref. [25] and in Fig. 1a and Fig. 2 of Ref. [24].

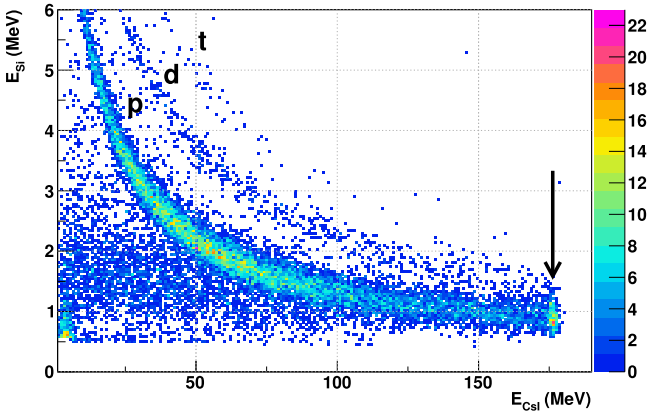

Fig. 4. The sum of the energies deposited in the two silicons vs. *LO* correlation for the crystal F2 in the case of 180 MeV proton beam. The vertical arrow indicates the proton elastic peak, while letters indicate the ridges of the Hydrogen isotopes. Only events with an energy deposition in Silicon detectors higher than the noise level are reported. Residual events due to γ-rays are present on the bottom left-hand side (see text).

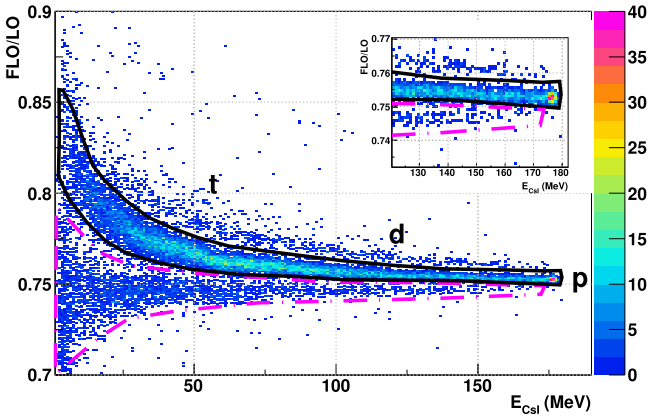

Fig. 5. Matrix $\frac{FLO}{LO}$ vs E_{CsI} for the crystal F2 measured at 180 MeV beam energy. The dotted-magenta contour is explained in the text. The black contour includes the properly identified protons. An expanded view of the region close to the elastic peak is also shown.

Fig. 4 shows the consequences of IED events in the ΔE–E correlation for one of the FAZIA detectors (F2) at 180 MeV proton energy. The sum of the energy deposited in the first two silicon layers is plotted versus the energy deposited in the CsI(Tl), according to the calibration of the *LO*. In the figure, one observes a long-extending ridge of well identified protons whose origin was already discussed (mainly scattering in the collimator). On the extreme right, the peak appears of elastically scattered protons (indicated by the arrow in the figure), characterized – amongst all identified protons – by the smallest energy deposit in silicon detectors and by the highest one in CsI(Tl). On the opposite extreme left-hand side an over-intensification of events is present, which, also according to GEANT4 simulations, are due to γ-rays produced by proton interactions in the iron collimator: Compton electrons are detected in Silicon and the associated photoelectrons in CsI(Tl). A contribution of deuterons and tritons ("d" and "t" in the figure) is also present, mainly ascribable to reactions in the ^{nat}Ti target without excluding those in the collimator. Events associated with IED of protons produce the wide band extending horizontally on the left hand side of the proton ridge.

The effect of IED events on PSA is less obvious than that present in the ΔE–E correlation. However, an insight may come from the known energy deposition profile for protons which presents a very sharp Bragg peak at the end of the pathlength. Therefore, since in CsI(Tl) the *fast* scintillation component is larger for higher stopping power values,

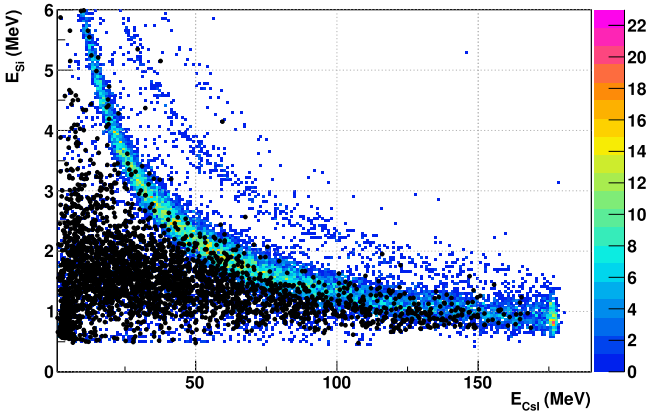

Fig. 6. ΔE–E correlation for protons at 180 MeV beam energy detected in the F2 telescope. The black points correspond to events falling within the dotted-magenta contour in Fig. 5.

the signal of an IED proton is expected to feature a reduced fast component with respect to a fully stopped proton depositing the same energy in the crystal. Before showing the associated results, a few words about the adopted method for PSA in CsI(Tl) are now in order. In fact, the identification of particles in these scintillators is usually obtained from the *FLO* vs *LO* correlation (or a linear combination thereof) – see for instance Ref. [5]. *FLO* and *LO* correspond to the amplitude of two different shapings of the CsI(Tl) light output, defined at the end of Section 2. In the present paper, we are following a slightly different approach, namely we use the $\frac{FLO}{LO}$ vs *LO* correlation. We have verified that this correlation permits a cleaner particle identification with respect to the other aforementioned approaches. The application of the procedure to the present case is shown in Fig. 5 for crystal F2 at 180 MeV proton beam energy. One clearly identifies the intense ridge of fully stopped protons (black contour) ending with the elastic peak region ("p" in the figure) and weaker ridges associated with fully stopped deuterons ("d") and tritons ("t"). More interesting for the present discussion is the appearance of events characterized by reduced $\frac{FLO}{LO}$ values (the dotted-magenta contour in the figure) with respect to the correct proton ridge. An expanded view around the elastic peak is also presented in the figure. It shows how events included in the dotted-magenta contour are merging in the ridge of properly identified protons. The events included in the dotted-magenta contour of the present correlations have been usually attributed to gamma-rays because the associated secondary electrons are indeed characterized by a smaller specific energy loss and consequently by a reduced *fast* component. Examples of this interpretation can be found in [3,25]. By using a ^{207}Bi gamma-source and exploiting events from cosmic muons, we performed a linear energy calibration of both F1 and F2 crystals for such low ionizing particles. The obtained calibration slope is about 4.4 ADU/MeV, close to the linear calibration coefficient obtained for protons.

This means that the dotted-magenta contour contains events, regardless to the detected particle species, up to an energy close to that of the elastic beam, i.e. 180 MeV. This actually excludes a sizeable gamma-ray contribution which is rather expected to populate the same region only at much smaller *LO* values (below 10 MeV in Fig. 5). Possible candidates for the higher energy region in the contour are therefore IED protons not having completed their pathlength in the crystal. In fact, such protons produce a light output typical of a low ionization density and consequently the fast (FLO) component is basically missing. In fact, this component is associated with the high ionization density characterizing the final part of the stopping process. This interpretation, which is also in agreement with the behavior presented in the expanded view in Fig. 5, is here put forward for the first time. A direct confirmation of this hypothesis is presented in Fig. 6 which shows the same

ΔE–E correlation of Fig. 4 where the black points correspond to events selected by the dotted-magenta contour of Fig. 5. The events in the dotted-magenta contour of the PSA do correspond to the events already interpreted as IED from the ΔE–E correlation. Events corresponding to interactions of neutrons, gamma-rays and cosmic rays possibly included in the dotted-magenta contour of Fig. 5 are characterized by Silicon energies within the noise level. Therefore they do not appear, apart from minor leaks, in Fig. 6, being excluded by the applied conditions on the Silicon energy. To summarize our findings: protons which do not complete their path in the CsI(Tl) produce a light output with a fast component similar to that of more energetic and less ionizing particles. This happens regardless of the particular mechanism which prevents the full energy deposition, i.e. either if the proton undergoes a reaction giving origin to undetected products or scatters out of the crystal. In any case, the associated $\frac{FLO}{LO}$ ratio falls below the proton locus in PSA, which belongs – let us stress this point – *to fully stopped particles.* Although the IED has been already reported in the past as the origin of background events in ΔE–E matrices, to our knowledge no attempt has ever been done before to connect it with the information coming from the PSA in CsI(Tl). We have now shown that such an approach permits not only to identify IED events, but also to avoid common misinterpretations of the events. As it will be shown in the next Section, the PSA in CsI(Tl) is also useful to determine the CsI(Tl) efficiency as a function of the proton energy, thanks to the identification of IED events.

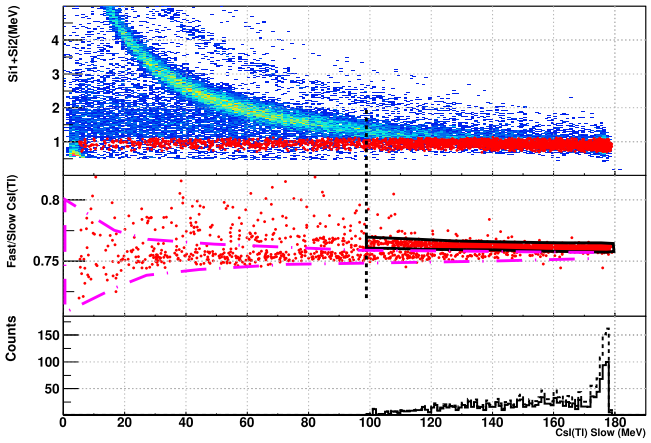

Fig. 7. Top panel: ΔE–E correlation for the F2 telescope already shown in Fig. 4, where the red points correspond to the selection of the $N_{in,el}$ events explained in the text. Middle panel: the same events shown as red points in the upper part are presented in the $\frac{FLO}{LO}$ vs E_{CsI} correlation. The colored contours are explained in the text. Bottom panel: energy distribution of the events with complete energy deposition selected by the black contour without (black line) and with (dotted line) efficiency correction (see text). Note that the beam energy is 180 MeV, but the low energy tail shifts the centroid of the distribution to ≈157 MeV. (For interpretation of the references to color in this figure legend, the reader is referred to the web version of this article.)

5. Study of the CsI(Tl) efficiency as a function of proton energy

In experiments at relatively high beam energies, the determination of the number of particles suffering IED in CsI(Tl) is indeed an issue to be solved. In fact, regardless of the chosen identification method (PSA or ΔE–E correlation), an energy dependent identification efficiency is introduced, leading to a distortion of the energy distributions [23,24]. To determine the energy dependence of such an efficiency, detailed simulations are needed, taking into account also the geometry of the detection system. For instance, a recent design study of the new crystals of the HiRA10 array [26] performed GEANT4 simulations in order to determine the effect of collisions (both elastic scattering and reactions) on the efficiency of the HiRA10 CsI(Tl) crystals. In the present paper, we are able to compare our experimental data with GEANT4 simulations tuned to the geometry of the FAZIA crystals. Both experimental data and simulation refer to the collimated geometry of the present experiment. The use of the ΔE–E and of the PSA correlations in CsI(Tl) provided us with an experimental method to evaluate the efficiency η of our telescopes for proton identification as a function of their energy. In fact, suppose that monochromatic protons of an energy E_{el} deposit in the silicon detectors an energy ΔE_{el}^{Si} and enter the crystal with an energy $E_{el}^{CsI} = E_{el} - \Delta E_{el}^{Si}$. In this case the efficiency η_{el} can be easily determined as:

$$\eta_{el} = \frac{N_{CED,el}}{N_{in,el}} = \frac{N_{CED,el}}{(N_{CED,el} + N_{IED,el})}$$

where $N_{in,el}$ represents the number protons entering the crystal with the energy E_{el}^{CsI} while $N_{CED,el}$ ($N_{IED,el}$) is the subset of these protons characterized by a complete (incomplete) energy deposition in the crystal. Therefore, in a ΔE–E telescope the selection of the $N_{in,el}$ protons entering the crystal with E_{el}^{CsI} can be performed by requiring the expected deposited energy ΔE_{el}^{Si} in the silicon detector(s), regardless of the residual energy measured in the crystal. The number $N_{CED,el}$ is obtained by simply selecting from this ensemble the subset of events corresponding to protons that correctly deposited both ΔE_{el}^{Si} in the silicon and E_{el}^{CsI} in the crystal, thus populating the elastic peak regions in both ΔE–E and PSA correlations.

Such an approach is impracticable in the present experiment because the energy distribution of protons stopped in the crystal extends to values lower than the elastic peak energy E_{el}. Consequently, as seen in Fig. 4, any selection of the deposited energy in silicons includes a non-vanishing fraction of lower energy protons. This happens for two connected reasons: a) the ΔE becomes very flat with increasing energy and b) the energy straggling and the finite energy resolution in silicon detectors make it difficult to exclude all protons impinging with $E < E_{el}$. Indeed, in order to impose a clean selection, we required the amplitude on both silicon detectors in front of the crystal to be within one standard deviation with respect to the mean values of ΔE_1 and ΔE_2 at the energy of the elastic peak. An additional cut is applied on the smallest energies deposited in the CsI(Tl) to totally remove the events due to the γ-rays otherwise present on the extreme left-hand side as in Fig. 4. The events corresponding to these selections are reported as red points in the upper part of Fig. 7. The figure shows the full ΔE–E correlation of the F2 telescope for 180 MeV protons beam energy. The total number of events N_{in} selected in this way provides an estimate of $N_{in,el}$. The middle panel of Fig. 7 shows how the same selected events, reported as red dots in the upper part, spread over the $\frac{FLO}{LO}$ vs E_{CsI} correlation.

Now the information contained in the $\frac{FLO}{LO}$ vs E_{CsI} correlation is apparent: the black contour shown in the middle panel of Fig. 7 includes protons which are correctly identified via both PSA and ΔE–E correlation. Those are the protons which spent their whole path length in the crystal and deposited in it their total kinetic energy. This contour is the same black contour drawn in Fig. 5, apart from the lower limit in energy which will be discussed shortly. The number N_{CED} of protons contained in this contour represents our estimate of $N_{CED,el}$. The vertical dotted line in Fig. 7 corresponds to the lower limit of the proton energy still compatible with the operated ΔE selection.

All the events outside the black contour represent IED events. Among them, special attention is paid to those included in the magenta (dotted line) contour. This contour is the same presented in Fig. 5 and it contains, as shown before, protons not fully stopped in the crystal which are characterized by a reduced *fast* component. One appreciates that an important fraction of IED protons belongs to this class of events.

Starting from our estimate of N_{CED} and N_{in} determined at all beam energies, it is possible to calculate the average experimental efficiency $\langle\eta\rangle = \frac{N_{CED}}{N_{in}}$ as a function of energy. The correct value for the average energy abscissa should be the centroid of the whole *inaccessible* original distribution of protons before suffering the IED losses. This distribution has been reconstructed, as a second step of the procedure, by correcting the experimental energy spectrum of the

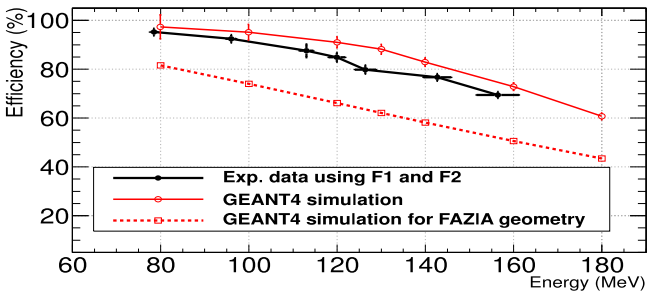

Fig. 8. (Color on line) The experimental identification efficiencies (black symbols) according to the selection described in the text compared with a GEANT4 simulation (red open dots) both in the collimated geometry. Open squares correspond to a GEANT4 simulation for the uncollimated geometry of FAZIA detectors. Connecting lines are used to guide the eye.

N_{CED} protons with the estimated efficiency determined as a function of energy in the first step. Given the small introduced correction (in the worst case few MeV), an iterative procedure was not necessary. In the bottom panel of Fig. 7, the experimental spectrum of N_{CED} is shown with a black line while the reconstructed spectrum is presented with a dotted black line. The procedure has been applied to both F1 and F2 telescopes providing compatible results. The so determined average experimental efficiencies are reported in Fig. 8 with black symbols. The connecting line is to guide the eye. The error bars on the Y-axis refer only to statistical uncertainties while the experimental bars in the energy axis represent the uncertainty associated with the cyclotron beam energy and with the procedure used to reconstruct the centroid. The experimental results of Fig. 8 are compared with a simulation performed with GEANT4 (red open symbols connected by a continuous red line to guide the eye). The sensitivity to the different parametrizations of the nuclear reactions in CsI(Tl) is small as shown in Ref. [26]. Anyway, we used the *FTFP_BERT_EMZ* [27,28] list to mimic the interaction of protons in the CsI(Tl), including also the *option4* for optimized low-energy electromagnetic interaction. The FAZIA crystal geometry in the collimated set-up is considered. The proton beam is simulated as a monochromatic source located at 40 cm far from the iron collimator. For the model, the errors are only statistical and reported on the Y-axis. No uncertainty is reported on the energy axis since in the simulation it is possible to calculate the efficiency by counting the labeled IED protons.

A reasonable agreement between the simulated and experimental results is observed. Specifically, GEANT4 satisfactorily reproduces the trend as a function of energy, although the average experimental efficiencies are systematically lower. Assuming the correctness of the simulations, this can be due to our experimental procedure which certainly suffers from the presence of the low energy tail in the energy distribution. We cannot exclude the presence of small biases due to possible inefficiencies of the selections performed with the ΔE–E and PSA correlations. They are difficult to calculate in a reliable way. This matter certainly deserves further investigation in future experiments. Finally, the dotted red line in Fig. 8 shows the results of the GEANT4 simulation when the whole front face of the detector is irradiated with protons emerging from a point source placed at 100 cm from the detector. This represents the estimated proton identification efficiency of the FAZIA telescopes as a function of energy in the normal operating conditions, when they are placed at such a distance from the target. The importance of the scattering in determining the identification efficiency is now apparent: the removal of any collimation implies that an increased fraction of particles impinges on the peripheral regions of the front face and is scattered out of the crystal.

6. Summary

Two CsI(Tl) crystals of the FAZIA array have been irradiated with protons of known energies from about 59 up to 180 MeV. The first purpose of the experiment was to verify the linearity of the energy calibration for protons in this energy range. The long flat top used for trapezoidal filtering excludes a significant ballistic deficit. We found the expected linearity of the *LO* vs. energy correlation below ~120 MeV, followed by a deviation (less than 4%) increasing at the highest measured energies, consistently with [19]. The amount and similarity of these deviations call for a deepening the study about their origin. Simulations and lab tests with gamma-ray sources are in progress suggesting that the non-linearity is due to the tapering of the crystals, as pointed out in [22].

A second goal was to study the effect of protons which undergo collisions in CsI(Tl) (scattering or reactions), producing an incomplete energy deposition (IED). We investigated the IED events, usually observed as a background in ΔE–E matrices, and we showed that, instead of populating the stopped proton ridge in the PSA correlation, they become spread out in a wide energy region, mainly located below the proton ridge, whose low energy part is usually expected to be populated just by gamma rays. To our knowledge, this observation was never pointed out before and corrects a common misinterpretation of these events. Here the effect is explained as the consequence of a reduction of the *fast* scintillation component due to the average lower specific energy loss of IED protons with respect to the fully stopped ones. Exploiting this behavior, we were able to deduce from the data the identification efficiency of CsI(Tl) crystals for correctly determining the proton yield as a function of energy. At the maximum investigated energy the efficiency drops to about 70%. The experimentally measured identification efficiency and the proposed interpretation find support from GEANT4 calculations, although further studies are required to find the origin of the remaining small – though significant – difference between experimental data and simulations. We will further investigate these topics by means of additional measurements with energetic protons by scanning the whole front face of the telescope to determine the identification efficiency for proton detection in realistic (uncollimated) experimental conditions, while continuing the comparison with GEANT4 simulations.

Declaration of competing interest

The authors wish to confirm that there are no known conflicts of interest associated with this publication and there has been no significant financial support for this work that could have influenced its outcome.

Acknowledgments

The authors would like to thank the CCB staff for providing high-quality beam. This work was supported by the Polish National Science Centre under Contracts No. 2014/14/M/ST2/00738 (COPIN-INFN Collaboration) and No. 2013/08/M/ST2/00257(COPIGAL).

References

[1] R. Bougault, et al., Eur. Phys. J. A 50 (2) (2014) 47.
[2] M. Bruno, et al., Eur. Phys. J. A 49 (10) (2013) 128.
[3] S. Wuenschel, et al., Nucl. Instr. and Meth. A 604 (3) (2009) 578.
[4] M. Wallace, et al., Nucl. Instrum. Methods A 583 (2) (2007) 302.
[5] J. Pouthas, et al., Nucl. Instrum. Methods A 357 (2–3) (1995) 418.
[6] S. Aiello, et al., Nuclear Phys. A583 (1995) C461.
[7] F. Benrachi, et al., Nuclear Phys. A 291 (1989) 137.
[8] J.B. Birks, The Theory and Practice of Scintillation Counters, Pergamon Press, Oxford, 1964, p. 439.
[9] M. Parlog, et al., Nucl. Instrum. Methods A 482 (3) (2002) 674.
[10] M. Parlog, et al., Nucl. Instrum. Methods A 482 (3) (2002) 693.
[11] L. Morelli, et al., Nucl. Instrum. Methods A 620 (2) (2010) 305.
[12] E. Valtonen, et al., Nucl. Instrum. Methods A 286 (1) (1990) 169.
[13] N. Colonna, et al., Nucl. Instrum. Methods A 321 (3) (1992) 529.
[14] F. Salomon, et al., J. Instrum. 11 (01) (2016) C01064.
[15] S. Valdré, et al., Nucl. Instrum. Methods A 930 (2019) 27.
[16] H. Hamrita, et al., Nucl. Instrum. Methods A 531 (2004) 607.

[17] V. Avdeichikov, et al., Nucl. Instrum. Methods A 439 (1) (2000) 158.
[18] A. Wagner, et al., Nucl. Instrum. Methods A 456 (3) (2001) 290.
[19] D. Dell'Aquila, et al., Nucl. Instrum. Methods A 929 (2019) 162.
[20] L. Bardelli, et al., Nucl. Instrum. Methods A 560 (2006) 517.
[21] L. Bardelli, et al., Nucl. Instrum. Methods A 560 (2006) 524.
[22] S. Diehl, et al., Nucl. Instrum. Methods A 857 (2017) 1.
[23] G. Poggi, et al., Nucl. Instrum. Methods A 324 (1993) 177.
[24] A. Siwek, et al., Nukleonika 47 (2002) 141.
[25] J. Lukasik, et al., Nucl. Instrum. Methods A 709 (2013) 120.
[26] P. Morfouace, et al., Nucl. Instrum. Methods A 848 (2017) 45.
[27] J. Allison, et al., Nucl. Instrum. Methods A 835 (2016) 186.
[28] http://geant4-userdoc.web.cern.ch/geant4-userdoc/UsersGuides/PhysicsListGuide/html.